IEEE Access
Multidisciplinary | Rapid Review | Open Access Journal

Received August 2, 2020, accepted September 2, 2020, date of publication September 14, 2020, date of current version September 24, 2020.

Digital Object Identifier 10.1109/ACCESS.2020.3023675

An Approach for Impedance Matrix Computation Considering Phase Transposition on Distribution Lines

HENRIQUE PIRES CORRÊA AND FLÁVIO HENRIQUE TELES VIEIRA
School of Electrical, Mechanical and Computer Engineering, Federal University of Goiás, Goiânia 74605-010, Brazil
Corresponding author: Henrique Pires Corrêa (pires_correa@ufg.br)

This work was supported by Coordenação de Aperfeiçoamento de Pessoal de Nível Superior (CAPES) under Grant Finance Code 001.

ABSTRACT A renewed interest in phase frame analysis of distribution systems has surfaced in recent literature due to rapid expansion of grid-integrated distributed generation and non-linear loads, whose grid imbalance-increasing effects require more detailed analysis and modeling of distribution systems for their proper assessment. In this paper, under motivation of such recent usage of phase frame components, we propose analytical equations for N-phase neutral-equipped line admittance matrix under transposition assumption. By using the proposed equations, we evaluate precision losses caused by using the transposition assumption for modeling three-phase four-wire distribution lines. Moreover, differently from previous works, we validate the transposition assumption and the admittance matrix values obtained for various combinations of cable type and line geometry. A relevant reason for analyzing transposition assumption in more detail is the fact that it may be useful in distribution system computations, due to its advantageous decoupling of symmetrical components. In this sense, the present work provides additional discussion and illustrative evaluations of the line transposition assumption, which may be useful for analyzing its applicability under different circumstances.

INDEX TERMS Power distribution lines, impedance, approximation error.

I. INTRODUCTION

Increasing attention has been recently directed towards the analysis of three-phase power systems in terms of phase frame components [1]–[7]. This trend can be justified by a greater interest in detailed modeling of distribution systems, whose unbalanced lines do not yield the main advantage obtained from usage of symmetrical components, namely decoupling of components in the sequence frame [8].

In general, effects of power system imbalance are significantly more pronounced at the distribution level, where they may not be ignored without incurring in large modeling errors. Among the phenomena that contribute to imbalance in distribution systems, we emphasize: single and two-phase laterals [9], three-phase line asymmetry and lack of transposition [10], [11], and integration of distributed generation [12]. Furthermore, imbalance itself contributes to other power quality problems, such as harmonic distortion [13]–[15].

The associate editor coordinating the review of this manuscript and approving it for publication was Taha Selim Ustun.

Given the significant imbalance of distribution systems, assuming perfect system balance during analysis is usually avoided. However, it cannot be denied that simplifications yielded by such assumptions, among which we emphasize component decoupling via symmetrical components, are highly desirable. Such decoupling can only be achieved if all line phases have equal self and mutual impedances [8], which would be true in case of phase symmetry or line transposition.

In this sense, interesting results were established by Kersting in [16]. It was shown via a case study that, in assuming the transposition of three-phase distribution lines, small errors were obtained in computing bus voltages, whereas errors for individual phase power losses were significant. Thus, it was suggested that assuming transposition in distribution systems is valid if the analysis is focused on voltage assessment.

It may be argued that such validation is insufficient, since the approximation error was evaluated for a single combination of cable type and conductor geometry. An additional evaluation of the method was carried out in [17], but the system under consideration had identical line geometry to that in [16]. To the best of our knowledge, no further work has attempted to test the method for different cases. Thus, the question concerning a more general validity of the method is left unanswered. In this sense, the objective of this work is providing further validation and discussion of the method via evaluation of new case studies.

A motivation for this work is the expansion of distributed generation integrated to distribution systems, which further contributes to system imbalance [18]. In fact, this has been a motivator for the renewed interest in three-phase modeling of distribution systems [19], [20]. A further evidence of this trend is the recent development of load flow solution methods tailored for explicit representation of neutral conductor and grounding [21]–[24]. In this context, we believe that evaluation of approximate techniques which may facilitate the application of sequence frame analysis is pertinent.

The remaining sections of this work are organized as follows. In Section II, the theoretical background regarding modeling of distribution lines and transposition are given; additionally, errors caused and computational advantages yielded by the transposition approximation are discussed. In Section III, a standard three-phase four-wire line model, which we adopt as reference for evaluating the transposition approximation, is presented. Subsequently, additional instances of distribution lines based on the original model, which are proposed in order to expand the validation of the transposition approximation, are presented and discussed. In Section IV, computational results corresponding to the previously presented evaluation instances are presented. Conclusions about the results are given in Section V.

II. THEORETICAL BACKGROUND

A. COMPUTATION OF LINE IMPEDANCE MATRIX

Consider a three-phase four-wire distribution line which connects buses designated by means of indexes i and j. We denote by $\hat{V}_i^r$ and $\hat{I}_{ij}^r$, respectively, the phasors of voltage in phase r of bus i and of current flowing from bus i to j in phase r, with the phase index $r \in \Phi = \{a, b, c, n\}$. Here, n designates neutral, whereas the remaining elements indicate system phases. In what follows, we adopt two approximate assumptions regularly used in distribution system analysis:

1) Ignoring shunt admittances, which is justified by negligible capacitance to ground due to short line lengths;
2) Considering zero-resistance grounding of the neutral conductor at both buses connected by the distribution line, which does not cause significant error due to neutral grounding impedances being small in practice.

Such assumptions allow representing the line via the equivalent circuit in Fig. 1, in which the grounded nodes imply $\hat{V}_i^n = \hat{V}_j^n = 0$ and $\boldsymbol{Z} = [z_{rs}]_{4\times4}$ is the line impedance matrix, with $r, s \in \Phi$. It is clear that mutual impedance does not depend on phase order, which implies that $\boldsymbol{Z}$ is symmetric. Furthermore, distribution lines are customarily built with equal conductors on all phases (but possibly different on neutral), thus $z_{aa} = z_{bb} = z_{cc}$. In this sense, we may restrict

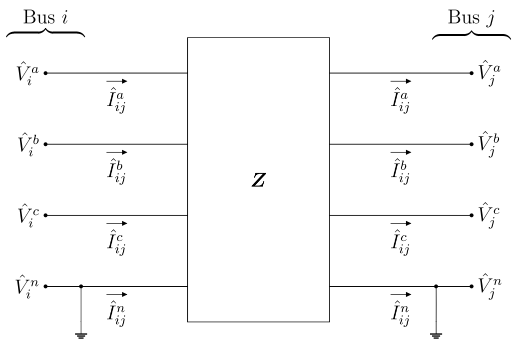

FIGURE 1. Equivalent circuit of distribution line.

the general impedance matrix to the form in (1):

$$\boldsymbol{Z} = \begin{bmatrix} z_{aa} & z_{ab} & z_{ac} & z_{an} \\ z_{ab} & z_{aa} & z_{bc} & z_{bn} \\ z_{ac} & z_{bc} & z_{aa} & z_{cn} \\ z_{an} & z_{bn} & z_{cn} & z_{nn} \end{bmatrix} \tag{1}$$

where the self and mutual impedances can be computed, in units of Ω/mile, by means of the following equations, which are known as the modified Carson equations [17]:

$$z_{rr} = [0.09530 + R_r] + j\left[0.12134 \cdot \left(\ln\frac{1}{D_{rr}} + f(\rho)\right)\right] \tag{2}$$

$$z_{rs} = 0.09530 + j\left[0.12134 \cdot \left(\ln\frac{1}{D_{rs}} + f(\rho)\right)\right] \tag{3}$$

$$f(\rho) = 7.6786 + \frac{1}{2} \cdot \ln\frac{\rho}{60} \tag{4}$$

where R_r is phase r cable resistance in Ω/mile, D_{rr} is the geometric mean radius of phase r conductors, D_{rs} is the geometric mean distance between conductors of phases r and s, both in feet, and ρ is earth resistivity in $\Omega \cdot$ meter. It must be noted that (2) to (4) presuppose grid operation at 60 Hz; however, analogous equations with different constants can be derived for any operation frequency [25].

It should be noted that (2) to (4) are often employed approximations to the original Carson equations for computing z_{rr} and z_{rs}. In such original equations, both real and imaginary parts of impedance are given by relatively cumbersome expressions, whose truncation of non-dominant terms yields the modified Carson equations. The most notable loss in precision due to truncation occurs in the real parts of z_{rr} and z_{rs}, which lose their dependence on ground resistivity. However, the imaginary parts of such impedances have a stronger dependence on ρ, which is maintained by means of the $f(\rho)$ term given in (4). For such reasons, the error caused by assumption that the resistive parts of z_{rr} and z_{rs} are constant with respect to ρ is small [25].

Let $\hat{\boldsymbol{V}}_i = [\hat{V}_i^r]_{1\times4}$ and $\hat{\boldsymbol{I}}_{ij} = [\hat{I}_{ij}^r]_{1\times4}$, $r \in \Phi$. Considering that $\hat{\boldsymbol{V}}_i - \hat{\boldsymbol{V}}_j = \boldsymbol{Z}\hat{\boldsymbol{I}}_{ij}$ and applying $\hat{V}_i^n = \hat{V}_j^n = 0$, a Kron-reduced impedance matrix $\boldsymbol{Z'} = [z'_{rs}]_{3\times3}$, $r, s \in \Phi' = \Phi - \{n\}$, is obtained. This matrix satisfies $\hat{\boldsymbol{v}}_i - \hat{\boldsymbol{v}}_j = \boldsymbol{Z'}\hat{\boldsymbol{i}}_{ij}$, where the reduced vectors $\hat{\boldsymbol{v}}_i = [\hat{V}_i^r]_{1\times3}$ and $\hat{\boldsymbol{i}}_{ij} = [\hat{I}_{ij}^r]_{1\times3}$, $r \in \Phi'$. The terms of $\boldsymbol{Z'}$ can be computed as functions of corresponding terms from $\boldsymbol{Z}$ [26]:

$$z'_{rs} = z_{rs} + \frac{z_{rn} z_{ns}}{z_{nn}} \tag{5}$$

It is worth mentioning that, despite the zero-resistance grounding assumption, the effects of neutral conductor and ground resistivity are incorporated into $\boldsymbol{Z'}$. This can be understood by observing that z'_{rs} is a function of z_{rs} and of impedance terms involving n, all of them being functions of ρ as in (2) to (4). Considering the symmetry and equal diagonal terms of $\boldsymbol{Z}$, as shown in (1), we conclude that the corresponding Kron-reduced matrix has the following form:

$$\boldsymbol{Z'} = \begin{bmatrix} z'_{aa} & z'_{ab} & z'_{ac} \\ z'_{ab} & z'_{aa} & z'_{bc} \\ z'_{ac} & z'_{bc} & z'_{aa} \end{bmatrix} \tag{6}$$

Some comments are now given concerning the exact computation of $\boldsymbol{Z}$ and $\boldsymbol{Z'}$, as given in (1) to (6). Firstly, it can be observed that storage of $\boldsymbol{Z}$ corresponds to storing eight complex numbers, whereas $\boldsymbol{Z'}$ requires storing four complex numbers. Generalizing to an N-phase system (e.g. $N = 6$ for the case of two lines in the same distribution pole [17]), the complex number storage requirements of both $\boldsymbol{Z}$ and $\boldsymbol{Z'}$ are $O(N^2)$. Considering that such impedance data are often used in load flow studies of systems comprising thousands of buses, reduction of storage requirements would be beneficial.

For the majority of load flow algorithms, it is necessary to obtain $\boldsymbol{Y} = \boldsymbol{Z}^{-1}$ or $\boldsymbol{Y'} = (\boldsymbol{Z'})^{-1}$ in order for the system admittance matrix to be computed. Given the $O(N^2)$ different elements of $\boldsymbol{Z}$, $\boldsymbol{Z'}$ and their corresponding inverses, it is impractical, even for $N = 3$, to derive and apply analytical equations for the elements of $\boldsymbol{Y}$ and $\boldsymbol{Y'}$. Hence, computation of these matrices is usually carried out via matrix inversion, which may be costly for a system with many lines.

In Section II-B, we discuss the transposition approximation and how the above-mentioned difficulties can be attenuated by means of its application. The error indexes that shall be used for evaluating the approximation are also defined.

B. ANALYTICAL COMPUTATION OF ADMITTANCE MATRIX VIA LINE TRANSPOSITION ASSUMPTION

By assuming that phases are transposed throughout the distribution line, the phase self impedances and mutual impedances between phases become equal to the average of those computed for the individual phases in the untransposed case. However, since the neutral conductor does not participate in transposition, its average mutual impedance is different from that of the phases, whereas its self impedance remains unaffected. Thus, the form of the approximate impedance matrix $\boldsymbol{Z_T}$ is:

$$\boldsymbol{Z_T} = \begin{bmatrix} z_s & z_m & z_m & z_n \\ z_m & z_s & z_m & z_n \\ z_m & z_m & z_s & z_n \\ z_n & z_n & z_n & z_{nn} \end{bmatrix} \tag{7}$$

where z_{nn} is the neutral self impedance as previously defined, and the remaining terms are given by:

$$z_s = \frac{1}{\#\Phi'} \sum_{r \in \Phi'} z_{rr} \tag{8}$$

$$z_m = \frac{1}{(\#\Phi')^2 - \#\Phi'} \sum_{r \in \Phi'} \sum_{s \in [\Phi' - \{r\}]} z_{rs} \tag{9}$$

$$z_n = \frac{1}{\#\Phi'} \sum_{r \in \Phi'} z_{rn} \tag{10}$$

where # denotes the number of elements in a set and we have $\#\Phi' = 3$, $\#\Phi = 4$ for the three-phase four-wire case. The corresponding Kron-reduced matrix $\boldsymbol{Z'_T}$ can be obtained by applying (5) and has the following form:

$$\boldsymbol{Z'_T} = \begin{bmatrix} z'_s & z'_m & z'_m \\ z'_m & z'_s & z'_m \\ z'_m & z'_m & z'_s \end{bmatrix} \tag{11}$$

Aside from the advantage of symmetrical component decoupling, it is clear that $\boldsymbol{Z_T}$ and $\boldsymbol{Z'_T}$ require less storage space than that of the exact impedance matrices. It can be seen that, for the three-phase case, the amount of complex numbers to be stored are reduced to four for $\boldsymbol{Z_T}$ and two for $\boldsymbol{Z'_T}$. In fact, once again generalizing to N-phase systems, it is clear that the storage requirement does not increase with the number of phases N, and thus is $O(1)$.

Due to the smaller number of different elements in $\boldsymbol{Z_T}$, simple analytical equations for the elements of $\boldsymbol{Y_T} = \boldsymbol{Z_T}^{-1}$ and $\boldsymbol{Y'_T} = (\boldsymbol{Z'_T})^{-1}$ can be derived. In this sense, we prove in the Appendix that the following theorem holds:

Theorem 1: Let $N = \#\Phi' = \#\Phi - 1$ and consider a *transposed* N-phase distribution line equipped with a neutral conductor. Also, let the elements of the $(N+1)$-th order $\boldsymbol{Y_T}$ and N-th order $\boldsymbol{Y'_T}$ follow the same subscript notation as that of (7) and (11). The elements of $\boldsymbol{Y_T}$ and $\boldsymbol{Y'_T}$ are given by:

$$y_s = \frac{z_{nn}[z_s + z_m(N-2)] - z_n^2(N-1)}{(z_m - z_s)\left\{N z_n^2 - z_{nn}[z_m(N-1) + z_s]\right\}} \tag{12}$$

$$y_m = -\frac{z_n^2 - z_m z_{nn}}{(z_m - z_s)\left\{N z_n^2 - z_{nn}[z_m(N-1) + z_s]\right\}} \tag{13}$$

$$y_n = \frac{z_n}{N z_n^2 - z_{nn}[z_m(N-1) + z_s]} \tag{14}$$

$$y_{nn} = -\frac{z_s + (N-1) z_m}{N z_n^2 - z_{nn}[z_m(N-1) + z_s]} \tag{15}$$

$$y'_s = \frac{z'_s + z'_m(N-2)}{(z'_s)^2 + z'_m[z'_s(N-2) - z'_m(N-1)]} \tag{16}$$

$$y'_m = -\frac{z'_m}{(z'_s)^2 + z'_m[z'_s(N-2) - z'_m(N-1)]} \tag{17}$$

where the admittances in (12) to (17) correspond to the respective impedance notations in (7) and (11).

To the best of our knowledge, (12) to (17) have not been derived in previous works concerning line transposition. The application of such equations when transposition is assumed can be useful, since their computational complexity is $O(1)$

due to not requiring matrix inversion routines, whose complexities necessarily increase with the number of phases N.

It is of interest to note that (2) to (5) and (8) to (10) are general, in the sense that they are applicable to an arbitrary number of phases. On the other hand, (1), (6), (7) and (11) are specific for the three-phase ($N = 3$) case.

III. PROPOSED CASE STUDIES

The reference feeder geometry selected for evaluating the transposition approximation is the IEEE overhead feeder #500 configuration [27]. This selection is due to such geometry being similar to the single configuration used in the original validation of the transposition assumption [16].

Such configuration is an established feeder geometry; it is adopted for modeling most three-phase overhead feeders that compose the IEEE test systems, in which multiple specifications of phase and neutral cables are used [27]. The cable data given in Table 1 are adopted as reference; such data correspond to the IEEE 4-bus system cable specification.

TABLE 1. Reference cable data.

Conductor type	Specification
Phase	336.4 kcmil 26/7 ACSR
Neutral	#4/0 AWG 6/1 ACSR

The reference geometry is illustrated in Fig. 2, alongside the values of mean geometric radii and resistances [8] of the adopted phase and neutral cable specifications.

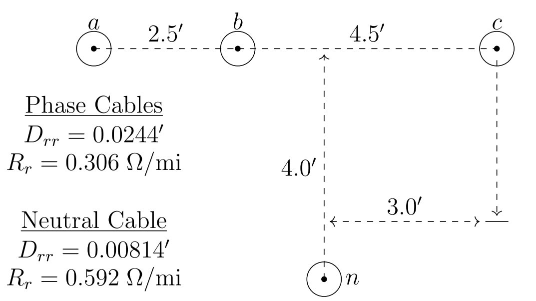

FIGURE 2. Conductor geometry and types for the base configuration.

In what follows, we propose three case studies which are modifications of the adopted reference geometry and cable data, allowing a more general validation of the transposition assumption. The influence of the following factors over approximation error is considered: cable specification, ground resistivity and height of neutral with respect to phases. Also, a more general analysis considering arbitrary positioning of neutral and one of the phases is carried out.

A. VARYING NEUTRAL HEIGHT RELATIVE TO FEEDER PHASES WITH CABLE TYPE AS PARAMETER

As a first extension of [16], impedance computations are carried out for fixed phase cables positions (as in Fig. 2) with variable height of the neutral cable with respect to the phase plane, which is henceforth denoted as Δh. For this case study, we adopt $\Delta h \in [0, 15']$ and parametrize the computations with three different cable specifications, all of which are used in the multiple existing IEEE test systems.

Let $C_r^{(i)} = \left(D_{rr}^{(i)}, R_r^{(i)}\right)$ denote the pair of mean geometric radius and resistance values associated to phase $r \in \Phi$, for a given cable specification $i \in \{1, 2, 3\}$. Also, $C^{(i)}$ denotes the data of all phases given in specification i. In Table 2, the adopted cable specifications and their respective $C^{(i)}$ labels are given. In Table 3, all values of R_r and D_{rr} are given, together with the IEEE test systems in which the cable instances are used. This case study is illustrated in Fig. 3, in which Γ_r denotes the set of all possible phase r cable specifications, i.e. $\Gamma_r = \left\{C_r^{(i)}, i \in \{1, 2, 3\}\right\}$.

TABLE 2. Cable specifications and labels (all cables are ACSR).

Label	Phase	Neutral
$C^{(1)}$	#4/0 AWG 6/1	#4/0 AWG 6/1
$C^{(2)}$	336.4 kcmil 26/7	#4/0 AWG 6/1
$C^{(3)}$	556.5 kcmil 26/7	#4/0 AWG 6/1

TABLE 3. Cable geometric mean radii (ft.) and resistances (Ω/mi).

Label	$C_r^{(i)}$ ($r \in \Phi'$)	$C_n^{(i)}$	IEEE
$C^{(1)}$	$(0.00814, 0.592)$	$(0.00814, 0.592)$	13
$C^{(2)}$	$(0.02440, 0.306)$	$(0.00814, 0.592)$	4, 123
$C^{(3)}$	$(0.03130, 0.186)$	$(0.00814, 0.592)$	13

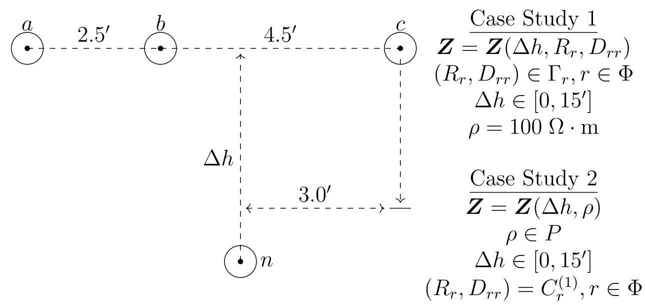

FIGURE 3. Illustration of first and second case studies.

The motivation for adopting a variable-position neutral arises from the fact that it is, in general, the element that introduces greatest asymmetry to feeder configurations. In fact, the neutral conductor is often the one with different diameter and not coplanar with the phases in practical installations (as is the case with the reference feeder adopted in this work). Thus, Δh can be interpreted as a measure both of neutral electromagnetic coupling and of system asymmetry. Intuitively, for increasing Δh the neutral coupling is reduced and thus system asymmetry decreases, which is expected to reduce the error due to assuming transposition.

B. VARYING NEUTRAL HEIGHT RELATIVE TO FEEDER PHASES WITH GROUND RESISTIVITY AS PARAMETER

In most works that involve computation of line impedance, it is assumed that earth resistivity ρ is equal to 100 $\Omega \cdot$ m.

Nevertheless, it is known that resistivity may vary in a relatively wide range depending on soil characteristics. The reasoning commonly used for assuming $\rho = 100\Omega \cdot \mathrm{m}$ is that the term $\frac{1}{2}\ln\frac{\rho}{60}$ does not dominate (4) in the usual resistivity range $100\ \Omega \cdot \mathrm{m} < \rho < 1000\ \Omega \cdot \mathrm{m}$ [25].

It must be observed that such considerations may not be immediately generalized to the present analysis. In fact, the above justification is applicable to the direct computation of $\boldsymbol{Z}$ and $\boldsymbol{Z'}$, whereas we want to analyze how ρ affects the error caused by substituting such matrices by their transposition approximation counterparts. This is non-trivial especially for the matrix $\boldsymbol{Z'}$, whose terms involve products of impedances each of which is affected by approximation error, as in (5).

Hence, this case study considers a feeder with identical geometry to that of the first case study, including a variable $\Delta h \in [0, 15']$, but with fixed cable specification $C^{(1)}$ and parametrization of cable impedance by resistivity. The values selected for resistivity are $\rho \in P = \{10, 100, 1000\}$ $(\Omega \cdot \mathrm{m})$; the case study is illustrated in Fig. 3.

C. VARYING NEUTRAL AND PHASE POSITIONS

Considering that the previous case studies encompass variable resistivity and cable type, we now propose a third case study in which approximation error is evaluated as a function of phase and neutral positions. To reduce the number of variables involved, we adopt a reference system xOy with fixed phases a and c on points $(0', 4')$ and $(7', 4')$, respectively; such relative positioning is identical to that of Fig. 2.

Phase b and neutral n are assigned arbitrary coordinates (x, y) and (x_n, y_n), respectively. Phase coordinates vary continuously in the domain $\mathcal{X} \times \mathcal{Y} =]0', 7'[\times [-3', 4']$, where the open interval is used to avoid superposition with phases a and c. The set $\mathcal{X}$ is such that phase b position is always between the fixed phases horizontally, whereas $\mathcal{Y}$ is specified to have the same range as $\mathcal{X}$, for the sake of simplicity.

In contrast, neutral coordinates may be assigned one of the points in the set $\mathcal{N} = \{(3.5', 0.5'), (6.0', 3.0')\}$. The first and second points were chosen to simulate, respectively, symmetrical and asymmetrical neutral placement with respect to the $\mathcal{X} \times \mathcal{Y}$ domain. Cable types and ground resistivity are assumed to be $C^{(1)}$ and $\rho = 100\Omega \cdot \mathrm{m}$, respectively. This case study is summarized in Fig. 4.

IV. RESULTS AND DISCUSSION

In what follows, the results of each proposed case study are sequentially presented and discussed. All results are given as plots of error indexes of the impedance matrices estimated via transposition assumption, with respect to their non-transposed counterparts. In each case study, the error curves are plotted as functions of continuous position variables (i.e., Δh, x and y) and parametrized by the discrete variables under consideration (i.e., cable type, ρ, x_n and y_n).

The adopted error indexes are defined in Section IV-A. All obtained results and their respective analyses are presented in sub IV-B to IV-D. In Section IV-E, a general discussion of the obtained results is carried out.

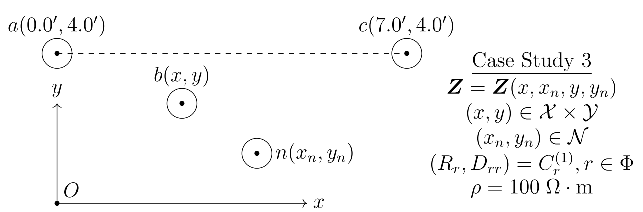

FIGURE 4. Illustration of third case study.

A. ERROR INDEXES

Recall that it was established in [16] that the transposition approximation is of interest mainly with regard to the computation of voltages. It is clear that voltage drop between line terminals is linear with respect to the impedance matrix itself. Thus, we abstract voltage and current from this analysis and evaluate impedance error directly. In this sense, we compute the absolute percentage errors for magnitude, phase angle, real part and imaginary part of each element in the matrix $\boldsymbol{Z}$:

$$e_{\mathcal{R}}(z_{rs}) = \frac{|\mathcal{R}\left[z_{rs} - z_{rs}|_T\right]|}{\mathcal{R}\left[z_{rs}\right]} \cdot 100\% \tag{18}$$

$$e_{\mathcal{I}}(z_{rs}) = \frac{|\mathcal{I}\left[z_{rs} - z_{rs}|_T\right]|}{|\mathcal{I}\left[z_{rs}\right]|} \cdot 100\% \tag{19}$$

$$e_{\mathcal{Z}}(z_{rs}) = \frac{|\,|z_{rs}| - |(z_{rs}|_T)|\,|}{|z_{rs}|} \cdot 100\% \tag{20}$$

$$e_{\Theta}(z_{rs}) = \frac{|\angle z_{rs} - \angle z_{rs}|_T|}{|\angle z_{rs}|} \cdot 100\% \tag{21}$$

where $(\cdot)|_T$ indicates usage of the transposition approximation and $\mathcal{R}$, $\mathcal{I}$, $\angle(\cdot)$, $|(\cdot)|$ are respectively: real part, imaginary part, phase angle and absolute value operators. Analogous impedance errors are computed for the Kron-reduced matrix and are denoted by $e'_{\mathcal{R}}(z'_{rs})$, $e'_{\mathcal{I}}(z'_{rs})$, $e'_{\mathcal{Z}}(z'_{rs})$ and $e'_{\theta}(z'_{rs})$. All absolute percentage errors are then used for computing the corresponding average absolute errors, which are:

$$E_{\mathcal{U}} = \frac{1}{(\#\Phi)^2}\sum_{r\in\Phi}\sum_{s\in\Phi} e_{\mathcal{U}}(z_{rs}) \tag{22}$$

$$E'_{\mathcal{U}} = \frac{1}{(\#\Phi')^2}\sum_{r\in\Phi'}\sum_{s\in\Phi'} e'_{\mathcal{U}}(z'_{rs}) \tag{23}$$

where $\mathcal{U}$ denotes any of the symbols: $\mathcal{R}$, $\mathcal{I}$, $\mathcal{Z}$ and Θ.

B. FIRST CASE STUDY

All average absolute errors for $\boldsymbol{Z}$ are plotted in Figs. 5(a) and 5(b), whereas the errors corresponding to $\boldsymbol{Z'}$ are given in Figs. 5(c) and 5(d). All errors are plotted as functions of Δh and with parameter $C_r^{(i)} \in \Gamma_r$, with $r \in \Phi$ and $i \in \{1, 2, 3\}$.

The results show that Δh has significant influence over approximation error, with higher values of neutral height being associated to smaller average errors. Such behavior could be reasonably expected, since a higher Δh implies smaller electromagnetic coupling between neutral and other conductors. This reduces the overall influence of the neutral

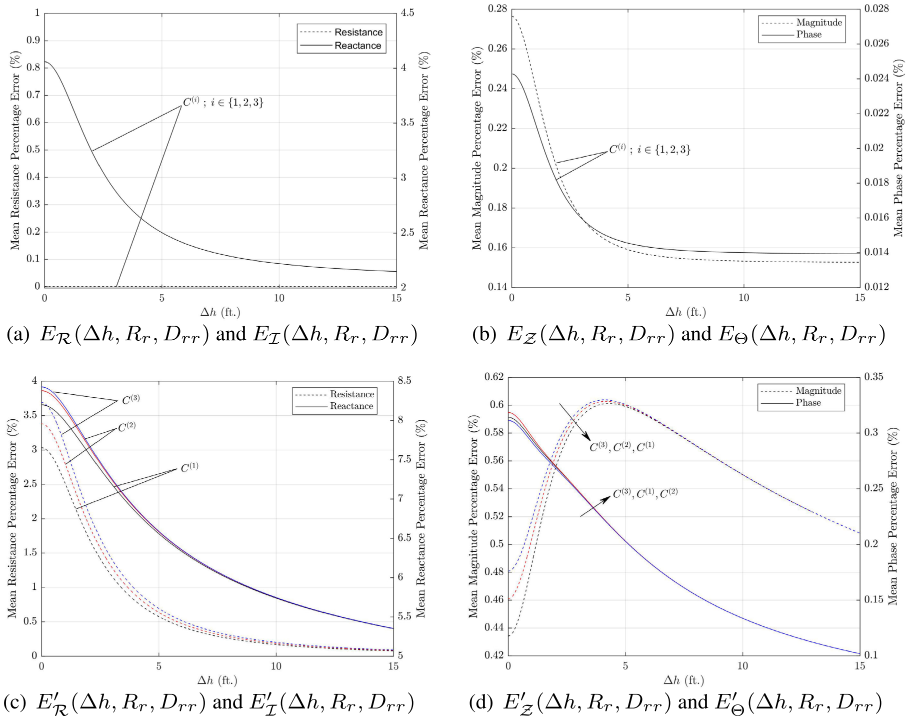

(a) $E_{\mathcal{R}}(\Delta h, R_r, D_{rr})$ and $E_{\mathcal{I}}(\Delta h, R_r, D_{rr})$ (b) $E_{\mathcal{Z}}(\Delta h, R_r, D_{rr})$ and $E_{\Theta}(\Delta h, R_r, D_{rr})$

(c) $E'_{\mathcal{R}}(\Delta h, R_r, D_{rr})$ and $E'_{\mathcal{I}}(\Delta h, R_r, D_{rr})$ (d) $E'_{\mathcal{Z}}(\Delta h, R_r, D_{rr})$ and $E'_{\Theta}(\Delta h, R_r, D_{rr})$

FIGURE 5. **Average absolute errors obtained in the first case study.**

conductor and increases system symmetry, which in turn decreases error due to less asymmetric information being disregarded when the transposition approximation is used. In general, it can be seen that all average errors underwent, approximately, twofold reductions when comparing the minimum and maximum values considered for Δh.

It is notable that $E_{\mathcal{R}} = 0$ for all Δh, which can be explained by the fact that all phase conductors have the same cable specification. Given that the series resistance of each phase depends on cable type and that all phases are equal in this respect, transposition is indifferent in this case. In contrast, $E'_{\mathcal{R}} \neq 0$ for all values of Δh, which may be explained by (5), where it can be seen that error in z'_{rs} is associated to the errors of z_{rs} and of the product $z_{rn}z_{ns}$ (z_{nn} is equal to neutral self-impedance and does not contribute to error). Thus, even with $E_{\mathcal{R}} = 0$, the product term is still subject to error, which implies $E'_{\mathcal{R}} \neq 0$.

Another salient feature of the results is the fact that mean absolute errors associated to $\mathbf{Z}$ do not depend on $C^{(i)}$, $i \in \{1, 2, 3\}$, which is not true for $\mathbf{Z'}$. This is a further effect of Kron reduction, which is now explained. The computation of $\mathbf{Z}$ by means of (2) to (4), with constant ρ, shows that the impedances' reactive parts depend solely on D_{rr} and D_{rs}. Considering that D_{rr} is equal for all phases, it does not contribute to transposition error. In addition, D_{rs} is not determined by cable type; for this reason, it does not depend on $C^{(i)}$. Hence, error for $\mathbf{Z}$ is also independent of $C^{(i)}$.

In opposition to the above reasoning for $\mathbf{Z}$, the results show that approximation error for $\mathbf{Z'}$ depends on $C^{(i)}$. This is a further consequence of Kron reduction via (5), due to which errors for individual impedances z'_{rs} depend on the product $z_{rn}z_{ns}$. As previously established, $E_{\mathcal{R}} = 0$, which means that the real parts of the individual terms of the product have no error. However, the product itself causes propagation of the individual imaginary part errors to the real and imaginary parts of its result. Finally, for $r = s$, the product depends on R_r and D_{rr}, making average error dependent on the cable specification $C^{(i)}$.

It should also be noted that, in spite of being influenced by $C^{(i)}$, average errors for $\mathbf{Z'}$ have a weak dependence on such parameter. This can be attributed to such dependence being only due to the diagonal terms of $\mathbf{Z'}$, namely z'_{rr}, $r \in \Phi'$. Furthermore, each set of error curves for the different $C^{(i)}$ converge towards each other for high Δh. This is due to the fact that, as $\Delta h \to \infty$, the term $z_{rn}z_{ns}$ in (5) tends to zero.

In terms of error magnitudes, the results of this case study suggest that the transposition approximation can be used if very high precision is not necessary when computing system voltages. Mean relative error for reactance was by far the highest, reaching above 8% in all cable types for $\Delta h = 0$. However, the lower relative errors of resistance (approximately 3% or less), coupled with the fact that resistance dominates reactance in distribution, keeps the magnitude and phase errors under 1%.

C. SECOND CASE STUDY

Analogously to the first case study, average absolute errors for $\mathbf{Z}$ are plotted in Figs. 6(a) and 6(b), whereas the errors

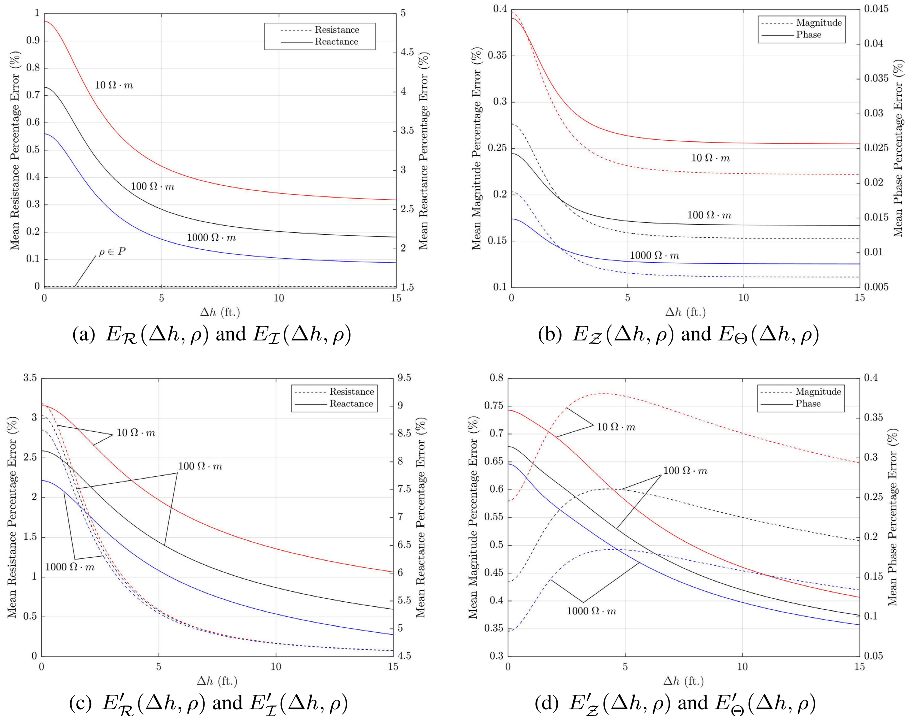

FIGURE 6. **Average absolute errors obtained in the second case study.**

corresponding to $\boldsymbol{Z}'$ are given in Figs. 6(c) and 6(d). All errors are plotted as functions of Δh with parameter $\rho \in P$.

It is immediate that ρ has a significantly more pronounced effect over reactance approximation error than $C^{(i)}$. In fact, the different values of ρ displace the reactance error curves in their entirety, whereas convergence to a common curve when $\Delta h \to \infty$ happened for variable $C^{(i)}$. Furthermore, a common $\boldsymbol{Z}$ reactance error curve for all $\rho \in P$ is not obtained, as was the case for $C_r^{(i)} \in \Gamma_r$, $r \in \Phi$. Contrariwise, convergence of the resistance error curves still happens for high Δh and the displacement between curves is much less pronounced. Furthermore, $E_{\mathcal{R}} = 0$ is still valid for all $\rho \in P$ due to the same reasons discussed in the first case study.

This difference between resistance and reactance errors may be explained from the fact that ρ only determines the imaginary part of reactances, as seen from (2) and (3). Hence, the resistance error curves follow essentially the same behavior as in the first case study: for $\boldsymbol{Z}$, error is null due to indifference of phase resistances with respect to transposition, whereas errors for $\boldsymbol{Z}'$ occur due to the $z_{rn}z_{ns}$ term in (5), whose effects decay as $\Delta h \to \infty$.

In a different manner, reactance errors are strongly dependent on $f(\rho)$, which is summed to the geometry-dependent (and thus prone to transposition error) term $\ln \frac{1}{D_{rs}}$ in (3). The results show that transposition error decreases for higher resistivity, which is explained as follows. From (4), it is clear that $\frac{df}{d\rho}(\rho) > 0$; thus, for greater ρ, the dominance of $f(\rho)$ in the sum $\left[\ln \frac{1}{D_{rs}} + f(\rho)\right]$ from (3) increases. Such increasing dominance tends to equalize the reactances of all z_{rs}, which in turn decreases error due to assuming transposition.

D. THIRD CASE STUDY

For conciseness, only relative errors for magnitude and phase are shown for this case study. In Figs. 7(a) to 7(d), error plots relative to $\boldsymbol{Z}$ and $\boldsymbol{Z}'$ are given for the symmetric neutral placement, whereas analogous results for asymmetric neutral are presented in Figs. 8(a) to 8(d).

The salient aspect of the obtained results is that approximation error grows rapidly due to proximity between two conductors (phase or neutral), with divergence occurring for coordinate superposition (which is impossible in practice).

This is an intuitively satisfactory result: if two of the conductors are in much closer proximity to each other than the remaining ones, it is implied that the feeder has a highly asymmetrical geometry. As a consequence of this, error penalties caused by assuming transposition are increased. It should be emphasized that the error surface peaks correspond to conductor superposition, which causes $\ln \frac{1}{D_{rs}} \to \infty$ in (3) and a consequent scaling of error towards infinity.

Comparison between the symmetric and asymmetric neutral cases shows that the main effect of neutral position is determining the neighborhood in which error divergence occurs. However, it is also important to note that errors (especially for magnitude) tend to be higher in the asymmetric case. This may also be explained via asymmetry, which tends to increase the transposition approximation error.

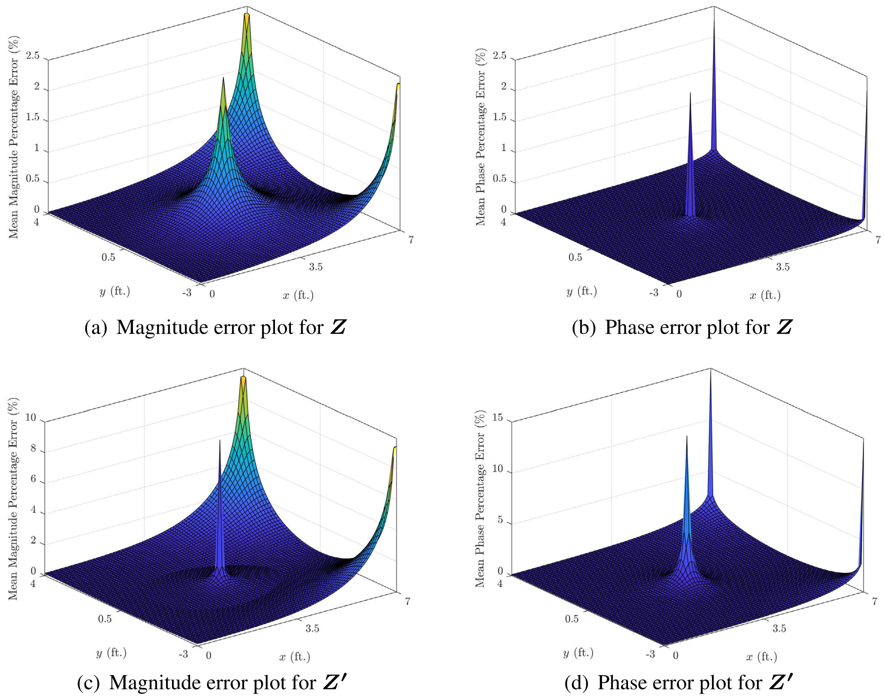

(a) Magnitude error plot for $\boldsymbol{Z}$ (b) Phase error plot for $\boldsymbol{Z}$

(c) Magnitude error plot for $\boldsymbol{Z}'$ (d) Phase error plot for $\boldsymbol{Z}'$

FIGURE 7. **Average absolute errors obtained in the third case study, considering symmetric neutral.**

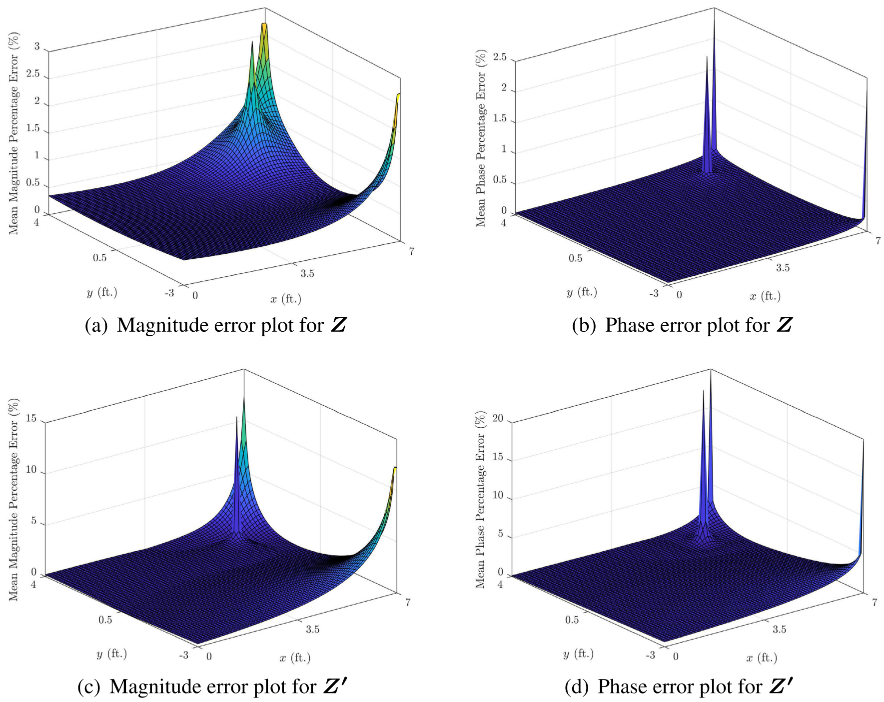

(a) Magnitude error plot for $\boldsymbol{Z}$ (b) Phase error plot for $\boldsymbol{Z}$

(c) Magnitude error plot for $\boldsymbol{Z}'$ (d) Phase error plot for $\boldsymbol{Z}'$

FIGURE 8. **Average absolute errors obtained in the third case study, considering asymmetric neutral.**

In a broader analysis, most general aspects of the error plots agree with those already discussed in the previous case studies. Among these, we mention greater relative errors for $\boldsymbol{Z}'$ when compared to $\boldsymbol{Z}$ and generally low errors, except in the neighborhood of divergence points.

E. DISCUSSION

In the following items, we summarize the salient features of the obtained results and analyses carried out in this paper.

- Despite being an often overlooked parameter in line impedance matrix modeling, grounding resistivity has significant influence in error incurred due to usage of the transposition approximation. Interestingly, in the proposed case studies, resistivity was found to have higher influence over error than the specification of phase and neutral cable types;
- Errors caused by the transposition approximation are higher for the Kron-reduced impedance matrix, when compared to its explicit-neutral counterpart. As shown in this work, this is due to further error propagation by a nonlinear impedance term (product of impedances) present in the Kron reduction equations;
- In terms of error, phase and neutral cable specification is unimportant for the explicit-neutral matrix. For the Kron-reduced case, it becomes irrelevant as the distances from neutral to the phases tends to infinity. It was shown that the former assertion is a consequence of all phase cables being usually equal to each other, whereas the latter is due to reduction of electromagnetic coupling between neutral and phases, which in turn decreases the impedance product term of Kron reduction;
- Relative positions of phase and neutral conductors have major influence over approximation error. Particularly, error increases rapidly when the distance between two conductors (either two phases or phase and neutral) becomes small with respect to other distances. In the extreme case of superposition, divergence occurs;
- In general, all obtained results suggest that the transposition approximation is applicable to practical distribution feeders. Clearly, this is a consequence of such feeders not usually presenting the characteristics (i.e. high asymmetry and/or proximity between two particular phases) for which error becomes high.
- Usage of transposition approximation may be advantageous in load flow studies due to its lower computational complexity and storage requirements in comparison to standard inversion of the impedance. In fact, analytic equations have been derived in this work for directly computing the impedance matrix inverse.

V. CONCLUSION

An extended analysis, with respect to previous works in the literature, of the transposition assumption and its influence over the impedance matrix of distribution lines was carried out. Multiple case studies were considered, in which error due to assuming transposition was evaluated as a function of line geometry, cable type and ground resistivity. The results corroborate previous assertions that the approximation error is low for practical systems, which suggests that the transposition approximation may be applied to voltage calculations.

A remarkable feature of the case study results is the fact that, aside from the dominance of line geometry, ground resistivity has significant influence over approximation error. This result is of interest because ground resistivity is an often overlooked parameter in modeling, for which standard values are usually assumed without further consideration. In this paper, we have also contributed with a derivation of general analytical equations for the N-phase, neutral-equipped line admittance matrix under transposition assumption. Given that a transposed line is assumed, using the derived equations reduces computational complexity by dispensing with the usual procedure of inverting the impedance matrix.

APPENDIX

DERIVATION OF ANALYTICAL EQUATIONS FOR THE ADMITTANCE MATRICES $\boldsymbol{Y_T}$ AND $\boldsymbol{Y'_T}$

Proof of Theorem 1: Let $\boldsymbol{Z_T}$ be the impedance matrix of an N-phase distribution feeder equipped with a neutral conductor. By matrix inversion, $\boldsymbol{Z_T}$ and $\boldsymbol{Y_T}$ have to satisfy:

$$\underbrace{\begin{bmatrix} z_s & z_m & \cdots & z_m & z_n \\ z_m & z_s & \cdots & z_m & z_n \\ \vdots & \vdots & \vdots & \vdots & \vdots \\ z_m & z_m & \cdots & z_s & z_n \\ z_n & z_n & \cdots & z_n & z_{nn} \end{bmatrix}}_{\boldsymbol{Z_T}} \underbrace{\begin{bmatrix} y_s & y_m & \cdots & y_m & y_n \\ y_m & y_s & \cdots & y_m & y_n \\ \vdots & \vdots & \vdots & \vdots & \vdots \\ y_m & y_m & \cdots & y_s & y_n \\ y_n & y_n & \cdots & y_n & y_{nn} \end{bmatrix}}_{\boldsymbol{Y_T}} = \boldsymbol{I_{NC1}} \tag{24}$$

where $\boldsymbol{I_{NC1}}$ is the $(N+1)$-th order identity matrix. Due to the particular structure of $\boldsymbol{Z_T}$ and $\boldsymbol{Y_T}$, the equality of their product with the identity matrix yields only five different equations, as will now be shown. In the following analysis, we consider the product of the k-th row of $\boldsymbol{Z_T}$ with the l-th column of $\boldsymbol{Y_T}$.

Firstly, for $1 \leq k, l \leq N$ and $k = l$, the N corresponding equations are identical and given by:

$$[z_s]y_s + [(N-1)z_m]y_m + [z_n]y_n = 1 \tag{25}$$

where coefficients of the desired admittance terms are highlighted with brackets. Now, for $1 \leq k, l \leq N$ and $k \neq l$, there are $N^2 - N$ identical equations expressed as:

$$[z_m]y_s + [z_s + (N-2)z_m]y_m + [z_n]y_n = 0 \tag{26}$$

For $1 \leq k \leq N$ and $l = N+1$, N equations are obtained:

$$[z_s + (N-1)z_m]y_n + [z_n]y_{nn} = 0 \tag{27}$$

In a similar manner, N equations are yielded for $k = N+1$ and $1 \leq l \leq N$:

$$[z_n]y_s + [(N-1)z_n]y_m + [z_{nn}]y_n = 0 \tag{28}$$

Finally, a single equation is given for $k = l = N+1$:

$$[Nz_n]y_n + [z_{nn}]y_{nn} = 1 \tag{29}$$

By summing the number of identical equations of each type, we arrive at the full $(N+1)^2$ equalities that are imposed by (24). The obtained equations compose a system of four variables with five equations; it must be shown that one of the equations is linearly dependent if a solution is to exist.

For conciseness, we do not carry out this procedure or the system solution in detail. However, it is of interest to indicate that linear dependence can be shown as follows: first, solve (27) and (29) for y_n and y_{nn}. Then, by inserting the obtained results in (26) and (28), it can be shown that such equations become identical to each other.

Hence, by disregarding (28), the following system of equations equivalent to (24) is obtained:

$$\begin{bmatrix} z_s & (N-1)z_m & z_n & 0 \\ z_m & z_s+(N-2)z_m & z_n & 0 \\ 0 & 0 & z_s+(N-1)z_m & z_n \\ 0 & 0 & Nz_n & z_{nn} \end{bmatrix} \begin{bmatrix} y_s \\ y_m \\ y_n \\ y_{nn} \end{bmatrix} = \begin{bmatrix} 1 \\ 0 \\ 0 \\ 1 \end{bmatrix} \tag{30}$$

The solution of this system yields (12) to (15).

An analogous derivation can be carried out for obtaining $\boldsymbol{Y}_T'$ by starting from the equality $\boldsymbol{Z}_T'\boldsymbol{Y}_T' = \boldsymbol{I}_N$. However, the corresponding system of equations may be directly obtained from (30) by omitting the last two variables, y_n and y_{nn}. Proceeding this way, the following system is obtained:

$$\begin{bmatrix} z_s' & (N-1)z_m' \\ z_m' & z_s'+(N-2)z_m' \end{bmatrix} \begin{bmatrix} y_s' \\ y_m' \end{bmatrix} = \begin{bmatrix} 1 \\ 0 \end{bmatrix} \tag{31}$$

whose solution yields (16) and (17). □

REFERENCES

[1] P. A. N. Garcia, J. L. R. Pereira, S. Carneiro, V. M. da Costa, and N. Martins, "Three-phase power flow calculations using the current injection method," *IEEE Trans. Power Syst.*, vol. 15, no. 2, pp. 508–514, May 2000.

[2] M. Bazrafshan and N. Gatsis, "Comprehensive modeling of three-phase distribution systems via the bus admittance matrix," *IEEE Trans. Power Syst.*, vol. 33, no. 2, pp. 2015–2029, Mar. 2018.

[3] J. Peppanen, C. Rocha, J. A. Taylor, and R. C. Dugan, "Secondary low-voltage circuit Models—How good is good enough?" *IEEE Trans. Ind. Appl.*, vol. 54, no. 1, pp. 150–159, Jan. 2018.

[4] M. F. AlHajri and M. E. El-Hawary, "Exploiting the radial distribution structure in developing a fast and flexible radial power flow for unbalanced three-phase networks," *IEEE Trans. Power Del.*, vol. 25, no. 1, pp. 378–389, Jan. 2010.

[5] H. Li, X. Yan, J. Yan, A. Zhang, and F. Zhang, "A three-phase unbalanced linear power flow solution with PV bus and ZIP load," *IEEE Access*, vol. 7, pp. 138879–138889, 2019.

[6] P. Caramia, G. Carpinelli, M. Pagano, and P. Varilone, "Probabilistic three-phase load flow for unbalanced electrical distribution systems with wind farms," *IET Renew. Power Gener.*, vol. 1, no. 2, pp. 115–122, Jun. 2007.

[7] P. Maffezzoni and G. Gruosso, "Complex-array-operation Newton solver for power grids simulations," *IEEE Access*, vol. 8, pp. 47984–47992, 2020.

[8] J. Grainger and W. Stevenson, *Power System Analysis* (McGraw-Hill Series in Electrical and Computer Engineering: Power and Energy). New York, NY, USA: McGraw-Hill, 2016.

[9] Y.-J. Kim, "Development and analysis of a sensitivity matrix of a three-phase voltage unbalance factor," *IEEE Trans. Power Syst.*, vol. 33, no. 3, pp. 3192–3195, May 2018.

[10] Z. Liu and J. V. Milanovic, "Probabilistic estimation of voltage unbalance in MV distribution networks with unbalanced load," *IEEE Trans. Power Del.*, vol. 30, no. 2, pp. 693–703, Apr. 2015.

[11] R. Yan and T. K. Saha, "Investigation of voltage imbalance due to distribution network unbalanced line configurations and load levels," *IEEE Trans. Power Syst.*, vol. 28, no. 2, pp. 1829–1838, May 2013.

[12] M. Zeraati, M. E. H. Golshan, and J. M. Guerrero, "Voltage quality improvement in low voltage distribution networks using reactive power capability of single-phase PV inverters," *IEEE Trans. Smart Grid*, vol. 10, no. 5, pp. 5057–5065, Sep. 2019.

[13] C. F. Nascimento, E. H. Watanabe, O. Diene, A. B. Dietrich, A. Goedtel, J. J. C. Gyselinck, and R. F. S. Dias, "Analysis of noncharacteristic harmonics generated by voltage-source converters operating under unbalanced voltage," *IEEE Trans. Power Del.*, vol. 32, no. 2, pp. 951–961, Apr. 2017.

[14] Y.-H. Lo, Y.-C. Chen, K. L. Lian, H. Karimi, and C.-Z. Wang, "An iterative control method for voltage source converters to eliminate uncharacteristic harmonics under unbalanced grid voltages for high-power applications," *IEEE Trans. Sustain. Energy*, vol. 10, no. 3, pp. 1419–1429, Jul. 2019.

[15] T. Zheng, E. B. Makram, and A. A. Girgis, "Evaluating power system unbalance in the presence of harmonic distortion," *IEEE Trans. Power Del.*, vol. 18, no. 2, pp. 393–397, Apr. 2003.

[16] W. H. Kersting and W. H. Phillips, "Distribution feeder line models," *IEEE Trans. Ind. Appl.*, vol. 31, no. 4, pp. 715–720, Jul. 1995.

[17] W. Kersting, *Distribution System Modeling and Analysis*. Boca Raton, FL, USA: CRC Press, 2016.

[18] L. R. Araujo, D. R. R. Penido, S. Carneiro, and J. L. R. Pereira, "A three-phase optimal power-flow algorithm to mitigate voltage unbalance," *IEEE Trans. Power Del.*, vol. 28, no. 4, pp. 2394–2402, Oct. 2013.

[19] A. M. M. Nour, A. Y. Hatata, A. A. Helal, and M. M. El-Saadawi, "Review on voltage-violation mitigation techniques of distribution networks with distributed rooftop PV systems," *IET Gener., Transmiss. Distrib.*, vol. 14, no. 3, pp. 349–361, Feb. 2020.

[20] Y. Ju, C. Chen, L. Wu, and H. Liu, "General three-phase linear power flow for active distribution networks with good adaptability under a polar coordinate system," *IEEE Access*, vol. 6, pp. 34043–34050, 2018.

[21] R. M. Ciric, L. F. Ochoa, and A. Padilha, "Power flow in distribution networks with Earth return," *Int. J. Electr. Power Energy Syst.*, vol. 26, no. 5, pp. 373–380, Jun. 2004.

[22] R. M. Ciric, A. P. Feltrin, and L. F. Ochoa, "Power flow in four-wire distribution networks-general approach," *IEEE Trans. Power Syst.*, vol. 18, no. 4, pp. 1283–1290, Nov. 2003.

[23] D. R. R. Penido, L. R. de Araujo, S. Carneiro, J. L. R. Pereira, and P. A. N. Garcia, "Three-phase power flow based on four-conductor current injection method for unbalanced distribution networks," *IEEE Trans. Power Syst.*, vol. 23, no. 2, pp. 494–503, May 2008.

[24] M. J. E. Alam, K. M. Muttaqi, and D. Sutanto, "A three-phase power flow approach for integrated 3-Wire MV and 4-Wire multigrounded LV networks with rooftop solar PV," *IEEE Trans. Power Syst.*, vol. 28, no. 2, pp. 1728–1737, May 2013.

[25] W. H. Kersting and R. K. Green, "The application of Carson's equation to the steady-state analysis of distribution feeders," in *Proc. IEEE/PES Power Syst. Conf. Expo.*, Mar. 2011, pp. 1–6.

[26] W. H. Kersting, "The computation of neutral and dirt currents and power losses," in *Proc. IEEE PES Power Syst. Conf. Expo.*, vol. 1, Oct. 2004, pp. 213–218.

[27] K. P. Schneider, B. A. Mather, B. C. Pal, C.-W. Ten, G. J. Shirek, H. Zhu, J. C. Fuller, J. L. R. Pereira, L. F. Ochoa, L. R. de Araujo, R. C. Dugan, S. Matthias, S. Paudyal, T. E. McDermott, and W. Kersting, "Analytic considerations and design basis for the IEEE distribution test feeders," *IEEE Trans. Power Syst.*, vol. 33, no. 3, pp. 3181–3188, May 2018.

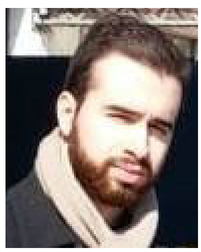

HENRIQUE PIRES CORRÊA received the bachelor's degree in electrical engineering and the master's degree in electrical and computer engineering from the Federal University of Goiás (UFG), Brazil, in 2017 and 2019, respectively, where he is currently pursuing the Ph.D. degree in electrical and computer engineering. His main research interests include power distribution networks, photovoltaic systems, and power system optimization.

FLÁVIO HENRIQUE TELES VIEIRA received the bachelor's degree in electrical engineering and the master's degree in electrical and computer engineering from the Federal University of Goiás (UFG), Brazil, in 2000 and 2002, respectively, and the Ph.D. degree in electrical engineering from the State University of Campinas (UNICAMP), in 2006. He is currently an Associate Professor with the School of Electrical, Mechanical and Computer Engineering (EMC), UFG. His main research interests include modeling and control of network traffic, communication networks, computational intelligence, and optimization applied to communication and power systems.